Functional interactions of the SPAK/OSR1 kinases with their upstream activator WNK1 and downstream substrate NKCC1

Alberto C. VITARI[1], Jacob THASTRUP, Fatema H. RAFIQI, Maria DEAK, Nick A. MORRICE, Håkan K. R. KARLSSON and Dario R. ALESSI

MRC Protein Phosphorylation Unit, School of Life Sciences, MSI/WTB complex, University of Dundee, Dow Street, Dundee DD1 5EH, Scotland, U.K.

The SPAK (STE20/SPS1-related proline/alanine-rich kinase) and OSR1 (oxidative stress-responsive kinase-1) kinases interact and phosphorylate NKCC1 (Na^+–K^+–$2Cl^-$ co-transporter-1), leading to its activation. Recent studies indicated that SPAK and OSR1 are phosphorylated and activated by the WNK1 [with no K (lysine) protein kinase-1] and WNK4, genes mutated in humans affected by Gordon's hypertension syndrome. In the present study, we have identified three residues in NKCC1 (Thr^{175}/Thr^{179}/Thr^{184} in shark or Thr^{203}/Thr^{207}/Thr^{212} in human) that are phosphorylated by SPAK and OSR1, and have developed a peptide substrate, CATCHtide (cation chloride co-transporter peptide substrate), to assess SPAK and OSR1 activity. Exposure of HEK-293 (human embryonic kidney) cells to osmotic stress, which leads to phosphorylation and activation of NKCC1, increased phosphorylation of NKCC1 at the sites targeted by SPAK/OSR1. The residues on NKCC1, phosphorylated by SPAK/OSR1, are conserved in other cation co-transporters, such as the Na^+–Cl^- co-transporter, the target of thiazide drugs that lower blood pressure in humans with Gordon's syndrome. Furthermore, we characterize the properties of a 92-residue CCT (conserved C-terminal) domain on SPAK and OSR1 that interacts with an RFXV (Arg-Phe-Xaa-Val) motif present in the substrate NKCC1 and its activators WNK1/WNK4. A peptide containing the RFXV motif interacts with nanomolar affinity with the CCT domains of SPAK/OSR1 and can be utilized to affinity-purify SPAK and OSR1 from cell extracts. Mutation of the arginine, phenylalanine or valine residue within this peptide abolishes binding to SPAK/OSR1. We have identified specific residues within the CCT domain that are required for interaction with the RFXV motif and have demonstrated that mutation of these in OSR1 inhibited phosphorylation of NKCC1, but not of CATCHtide which does not possess an RFXV motif. We establish that an intact CCT domain is required for WNK1 to efficiently phosphorylate and activate OSR1. These data establish that the CCT domain functions as a multipurpose docking site, enabling SPAK/OSR1 to interact with substrates (NKCC1) and activators (WNK1/WNK4).

Key words: cation co-transporter, Gordon's syndrome, hypertension, protein kinase, pseudohypoaldosteronism type II, STE20/SPS1-related proline/alanine-rich kinase (SPAK).

INTRODUCTION

The protein kinases SPAK (STE20/SPS1-related proline/alanine-rich kinase) and OSR1 (oxidative stress-responsive kinase-1) were originally identified through their ability to interact with and stimulate the activity of NKCC1 (Na^+–K^+–$2Cl^-$ co-transporter) [1,2]. SPAK and OSR1 are 68% identical in sequence, possess a highly similar kinase catalytic domain as well as a CCT (conserved C-terminal) domain, comprising 92 amino acids that are 79% identical in sequence. The CCT domain interacts with RFXV (Arg-Phe-Xaa-Val) motifs in NKCC1 [1] as well as other potential binding partners [3,4]. Recent studies indicate that the WNK1 [with no K (lysine) protein kinase-1] and WNK4 enzymes phosphorylate and activate the SPAK and OSR1 protein kinases [5,6]. Mutations in the genes encoding WNK1 and WNK4 enzymes are found in families with an inherited hypertension and hyperkalaemia (elevated plasma K^+) disorder termed Gordon's syndrome or pseudohypoaldosteronism type II [7]. The WNK1 and WNK4 protein kinases phosphorylate SPAK and OSR1 at their T-loop residue (Thr^{233} in SPAK, Thr^{185} in OSR1) in addition to a non-catalytic serine residue lying in a conserved motif between the catalytic and CCT domain (Ser^{373} in SPAK, Ser^{325} in OSR1) [6]. Mutational analysis indicates that phosphorylation of the T-loop in SPAK and OSR1 rather than the phosphorylation of the serine residue mediates activation by WNK1 [6]. Consistent with this, mutation of the T-loop threonine residue, phosphorylated by WNK1/WNK4, to a glutamate residue to mimic phosphorylation increases the basal activity of OSR1 [6] and SPAK (A. C. Vitari, unpublished work) over 10-fold and prevents further activation by WNK1. In the present study, we have mapped the residues on NKCC1 that are phosphorylated by SPAK and OSR1 and we have shown that endogenous NKCC1 phosphorylation at these sites is increased in response to hyperosmotic stress in cells. Furthermore, we have developed a peptide substrate that can be employed to easily assess the activity of these kinases. We have also characterized the binding properties of the CCT domain and establish that it plays an important role in regulating the activation of SPAK/OSR1 by WNK1 as well as the phosphorylation of SPAK/OSR1 substrates such as NKCC1.

MATERIALS AND METHODS

Materials

Sequencing-grade trypsin and protease-inhibitor cocktail tablets were from Roche. Dialysed foetal bovine serum and other

tissue-culture reagents were from Life Technologies. [γ-^{32}P]ATP, streptavidin–Sepharose high-performance and glutathione–Sepharose 4B were from Amersham Biosciences. Colloidal Blue staining kit was from Invitrogen. Tween 20 was from Sigma. Nonidet P40 was from Fluka. P81 phosphocellulose paper was from Whatman. GST (glutathione S-transferase)–PreScission protease was expressed and purified from *Escherichia coli* using plasmids kindly provided by Professor John Heath (School of Biosciences, University of Birmingham, Birmingham, U.K.). All peptides were synthesized by Dr Graham Bloomberg (Molecular Recognition Centre, University of Bristol School of Medical Sciences, Bristol, U.K.). Streptavidin-coated (SA) sensor chips were from BiaCore AB (Stevenage, Herts., U.K.).

General methods, buffers and DNA constructs

Tissue culture, transfection, immunoblotting, restriction-enzyme digests, DNA ligations and other recombinant DNA procedures were performed using standard protocols. All mutagenesis steps were carried out using the QuikChange® site-directed mutagenesis kit (Stratagene) using KOD polymerase from *Thermococcus kodakaraensis* (Novagen). DNA constructs used for transfection were purified from *E. coli* DH5α cells using Qiagen plasmid Mega or Maxi kit according to the manufacturer's protocol. All DNA constructs were verified by DNA sequencing, which was performed by the Sequencing Service, School of Life Sciences, University of Dundee, Dundee, Scotland, U.K., using DYEnamic ET terminator chemistry (Amersham Biosciences) on Applied Biosystems automated DNA sequencers. Lysis buffer was 50 mM Tris/HCl, pH 7.5, 1 mM EDTA, 1 mM EGTA, 1 % (w/w) Nonidet P40, 1 mM sodium orthovanadate, 50 mM NaF, 5 mM sodium pyrophosphate, 0.27 M sucrose, 1 mM DTT (dithiothreitol) and Complete™ protease-inhibitor cocktail (one tablet per 50 ml). Buffer A was 50 mM Tris/HCl, pH 7.5, 0.1 mM EGTA and 1 mM DTT. Sample Buffer was 1× NuPAGE® LDS (lithium dodecyl sulphate) sample buffer (Invitrogen) containing 1 % (v/v) 2-mercaptoethanol. For expression of proteins in *E. coli*, pGEX-6P-1 constructs were transformed into *E. coli* BL21 cells, expressed and purified as described previously [6]. For expression of proteins in HEK-293 (human embryonic kidney) cells, this was undertaken as described previously [6]. The cloning of human WNK1 [8], SPAK, OSR1 and a fragment corresponding to amino acids 1–260 of dogfish shark NKCC1 [6] were described previously.

Mapping phosphorylation sites on NKCC1

The activation assay mixtures were set up in a total volume of 25 μl of buffer A, containing 0.25 μM GST–WNK1-(1–661) (expressed in *E. coli*), 5 μM GST–SPAK or 5 μM GST–OSR1 (expressed in *E. coli*), 10 mM MgCl$_2$ and 0.1 mM non-radioactive ATP. After incubation for 40 min at 30°C, 5 μl of the activation assay mix was transferred to 20 μl of buffer A containing 6.25 μM NKCC1-(1–260) expressed in *E. coli*, 10 mM MgCl$_2$ and 0.1 mM [γ-^{32}P]ATP ($\sim$3000 c.p.m./pmol). After incubation for 40 min at 30°C, incorporation of phosphate was determined following electrophoresis of samples on 10 % NuPAGE® Bis-Tris gels and autoradiography of Coomassie Blue-stained gels. The protein bands corresponding to NKCC1 were excised, and phosphate incorporation was quantified on a PerkinElmer liquid-scintillation counter. Following tryptic digestion, > 87 % of the ^{32}P radioactivity incorporated in the gel bands was recovered and the samples were chromatographed on a reverse-phase HPLC Vydac 218TP5215 C$_{18}$ column (Separations Group) as described in the legend to Figure 1. Fractions corresponding to the major

^{32}P-containing peaks were analysed using an Applied Biosystems 4700 proteomics analyser [MALDI–TOF/TOF (matrix-assisted laser-desorption ionization–tandem time-of-flight)] and solid-phase Edman degradation on an Applied Biosystems 494C sequenator of the peptide coupled to Sequelon-AA membrane (Milligen) [9].

In vitro NKCC1 phosphorylation reactions

Assays were set up in a total volume of 25 μl of buffer A containing 1 μM GST–[T185E]OSR1 or GST–[T233E]SPAK expressed in *E. coli*, 5 μM NKCC1-(1–260), GST–NKCC1-(1–260) or GST–[T175A/T179A/T184A]NKCC1-(1–260), 10 mM MgCl$_2$ and 0.1 mM [γ-^{32}P]ATP ($\sim$300 c.p.m./pmol). After incubation for 40 min at 30°C, incorporation of phosphate was determined as described above.

OSR1 kinase assays employing CATCHtide (<u>cat</u>ion <u>ch</u>loride co-<u>t</u>ransporter peptide substrate) or NKCC1-(1–260)

Assays were set up in a total volume of either 50 μl (CATCHtide assay) or 25 μl (NKCC1 assay) in buffer A containing 10 mM MgCl$_2$, 0.1 mM [γ-^{32}P]ATP ($\sim$300 c.p.m./pmol), 0.08–0.5 μM GST–[T185E]OSR1, 300 μM CATCHtide (RRHYYYDTHTNT-YYLRTFGHNTRR) or 5 μM NKCC1-(1–260). After incubation for 10–60 min at 30°C, the reaction mixture was applied on to P81 phosphocellulose paper, the papers were washed in phosphoric acid and incorporation of ^{32}P radioactivity into CATCHtide was quantified as described previously [10]. For the NKCC1 assay, the reaction was stopped by the addition of SDS sample buffer and phosphorylation of NKCC1 was assessed as described above following SDS/PAGE (10 % Bis-Tris).

Antibodies

For immunoblotting of WNK1, an antibody raised in sheep against WNK1 protein encompassing residues 61–661 expressed in *E. coli* was used [8]. For the immunoprecipitation of WNK1 (see Figure 8), we employed an antibody raised against the C-terminus of human WNK1 (residues 2360–2382: QNFNISNLQ-KSISNPPGSNLRTT) [8]. For immunoblotting of phosphorylated NKCC1 (see Figure 2), an antibody raised in sheep against a peptide encompassing residues 198–217 of human NKCC1 phosphorylated at Thr^{203}, Thr^{207} and Thr^{212} was used (HYYYDpTHT-NpTYYLRpTFGHNT). For the immunoprecipitation and immunoblotting of NKCC1 from HEK-293 cells in Figure 2(B), an antibody raised in sheep against shark NKCC1-(1–260) expressed and purified from *E. coli* was used. T4 anti-NKCC1 mouse monoclonal antibody was purchased from Developmental Studies Hybridoma Bank (Iowa University, Iowa City, IA, U.S.A.) and used for immunoblotting of NKCC1 as shown in Figures 4 and 5. Mouse monoclonal antibodies recognizing GST were purchased from Sigma (#G1160). Secondary antibodies coupled to fluorophores were from Molecular Probes and Rockland Technologies.

Immunoblotting

Samples were heated in sample buffer, subjected to SDS/PAGE (3–8 % Tris/acetate) and transferred on to nitrocellulose membranes. Membranes were blocked for 5 min in TBST [Tris-buffered saline with Tween 20; 50 mM Tris/HCl (pH 7.5), 0.15 M NaCl and 0.2 % Tween 20], containing 10 % (w/v) dried skimmed milk. The membranes were then incubated for 16 h at 4°C in TBST containing 10 % (w/v) dried skimmed milk with 0.5 μg/ml anti-WNK1 antibody, 2 μg/ml anti-phospho-NKCC1 antibody,

5 μg/ml anti-NKCC1-(1–260) antibody, 10 000-fold dilution for anti-GST antibody or 100 μg/ml ascites containing monoclonal T4 anti-NKCC1 antibody. Detection was performed using fluorophore-conjugated antibody and a Li-Cor Odyssey® IR imaging system.

Affinity-purification of SPAK and OSR1 employing the biotin–RFQV peptide

A 1 mg portion of clarified HEK-293 cell lysate expressing forms of GST–OSR1 (see Figure 6B) or 10 mg of untransfected HEK-293 cell lysate (see Figure 6D) was incubated with 3 μg of the indicated biotinylated peptide for 15 min at 4 °C. A 10 μl aliquot of streptavidin beads equilibrated in lysis buffer was added. After 15 min of incubation at 4 °C under gentle agitation, the beads were washed twice with lysis buffer containing 0.5 M NaCl, followed by two washes with buffer A. The beads were boiled in 1× NuPAGE® LDS sample buffer, and the samples were subjected to SDS/PAGE (10 % Bis-Tris). The gels were either transferred on to nitrocellulose membranes for immunoblotting or stained with Colloidal Blue staining kit according to the manufacturer's protocol and were processed for MS fingerprinting.

Immunoprecipitation of endogenous WNK1 and NKCC1

HEK-293 cells grown on 10-cm-diameter dishes were lysed in 0.5 ml of lysis buffer and were clarified by centrifugation at 14 000 g for 5 min. For immunoprecipitations, 0.5 mg (WNK1) or 2 mg (NKCC1) of lysate was incubated at 4 °C for 1 h with 5 μl of Protein G–Sepharose beads conjugated to 5 μg of anti-(WNK1 C-terminus) antibody, 1.5 μg of anti-NKCC1-(1–260) antibody or the equivalent amount of pre-immune antibody. The immunoprecipitates were washed twice with lysis buffer containing 0.5 M NaCl, and twice with buffer A.

Biacore analysis

Binding was analysed in a BiaCore 3000 system. The indicated biotinylated peptides were bound to an SA sensor chip (400 response units). The indicated concentrations of bacterially expressed wild-type and mutant forms of GST–OSR1 fusion protein in HBS-EP [Hepes-buffered saline with EDTA and polysorbate 20; 10 mM Hepes, pH 7.4, 0.15 M NaCl, 3 mM EDTA and 0.005 % (v/v) polysorbate 20], were injected over the immobilized peptides at a flow rate of 30 μl/min. Interactions between each peptide and the GST–OSR1 forms were analysed and steady-state binding was determined at each concentration. Dissociation of GST–OSR1 forms from each peptide was monitored over 90 s. Regeneration of the sensor chip surface between each injection was performed with three consecutive 5 μl injections of a solution containing 10 mM NaOH and 1 M NaCl.

RESULTS

Mapping residues in NKCC1 that are phosphorylated by SPAK and OSR1

To define the residues in the N-terminal regulatory domain of NKCC1 that are phosphorylated by SPAK and OSR1, we employed a fragment of shark NKCC1 encompassing residues 1–260 that SPAK and OSR1 are known to phosphorylate efficiently [2,5,6]. Under the conditions employed, NKCC1-(1–260) was phosphorylated by active SPAK or OSR1 to ∼ 0.15 mol of phosphate/mol, digested with trypsin and chromatographed on a C_{18} column to isolate ^{32}P-labelled phosphopeptides (Figures 1A and 1B). Both profiles were similar, revealing the presence of

two major phosphopeptides termed P1/P3 and P2/P4. MS and Edman sequencing established the identity of P1/P3 as a peptide doubly phosphorylated at Thr[175] and Thr[179] (corresponding to Thr[203] and Thr[207] in human NKCC1; see Figure 3A), and P2/P4 as a peptide phosphorylated at Thr[184] (corresponding to Thr[212] in human NKCC1; see Figure 3A). We next assessed how mutation of these residues affected the phosphorylation of NKCC1-(1–260). Individual mutation of Thr[175], Thr[179] or Thr[184] to alanine moderately reduced phosphorylation of NKCC1 by SPAK (Figure 1C) and OSR1 (Figure 1D), whereas a mutant of NKCC1 in which all three residues were replaced by alanine was no longer phosphorylated by either SPAK (Figure 1C) or OSR1 (Figure 1D).

Phosphorylation of endogenous NKCC1

In order to study whether endogenous NKCC1 was phosphorylated on the residues that are phosphorylated by SPAK/OSR1, we raised a phosphospecific antibody against a peptide encompassing residues 198–217 of human NKCC1 phosphorylated on Thr[203], Thr[207] and Thr[212]. This antibody recognized NKCC1-(1–260) only after it was phosphorylated by active OSR1 *in vitro* (Figure 2A). A mutant form of NKCC1-(1–260) in which Thr[203], Thr[207] and Thr[212] were replaced by alanine was not recognized by the anti-phospho-NKCC1 antibody after incubation with active OSR1 and MgATP (Figure 2A). We next assessed whether endogenous NKCC1 was phosphorylated at the residues targeted by SPAK and OSR1. Previous work demonstrated that hyperosmotic stress such as that induced by sorbitol results in hyperphosphorylation and activation of NKCC1 [11]. To verify whether sorbitol increased phosphorylation of endogenous NKCC1 at the sites phosphorylated by SPAK and OSR1, we treated HEK-293 cells in the presence or absence of 0.5 M sorbitol and immunoblotted cell lysates or NKCC1 immunoprecipitates with the anti-phospho-NKCC1 antibody. These data demonstrate that sorbitol increased phosphorylation of NKCC1 2-fold (Figure 2B).

Generation of a peptide substrate for SPAK and OSR1

A peptide encompassing residues 198–217 of human NKCC1 (almost identical with residues 170–189 of shark NKCC1; Figure 3A) in which two arginine residues were added to the N- and C-termini to increase solubility and ability to interact with P81 phosphocellulose paper was generated. This peptide was phosphorylated by the active [T185E]OSR1 mutant (Figure 3B), with a K_{m} of 330 μM and a V_{max} of 5.7 units/mg. Similar results were obtained using the active [T233E]SPAK mutant (not shown). This peptide was termed CATCHtide, and can be employed to assess SPAK/OSR1 activity in a straightforward manner, using the assay described in the Materials and methods section.

Residues of the CCT domain of SPAK and OSR1 required for binding to NKCC1 and WNK1

Previous studies using yeast two-hybrid analysis indicated that the CCT domain of SPAK and OSR1 bound to NKCC1 [1], as well as WNK4 [3,4], through an RFXV motif. Consistent with this, we found that full-length SPAK (547 amino acids long) or OSR1 (527 amino acids long) or the isolated CCT domain of these enzymes, when expressed in HEK-293 cells, interacted with endogenously expressed NKCC1 (Figure 4A). We were unable to detect endogenously expressed WNK4 in HEK-293 cells, but found that endogenously expressed WNK1 that possesses five RFXV motifs, interacted with the CCT domain-containing fragments of SPAK and OSR1 (Figure 4A). Mutant forms of SPAK and OSR1 lacking the CCT domain failed to bind NKCC1 or WNK1 (Figure 4A). To determine which residues on the CCT
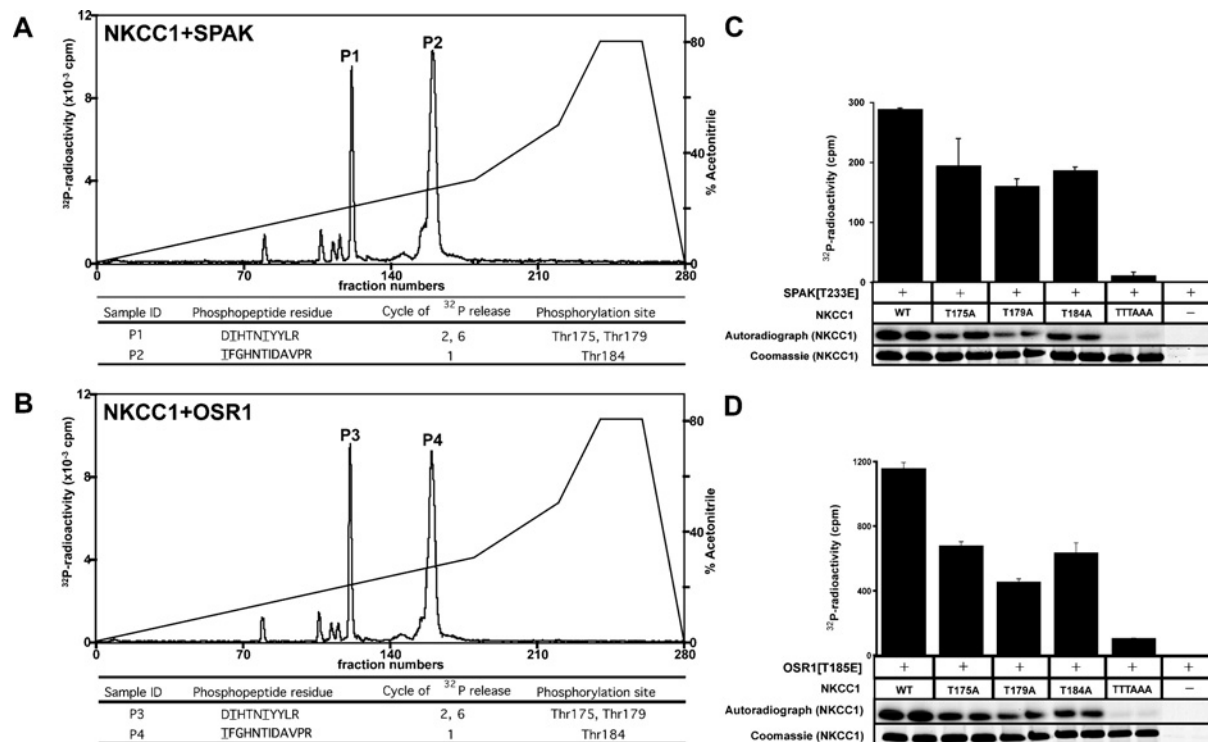
Figure 1   Sites on NKCC1 phosphorylated by SPAK and OSR1

(**A**) Shark NKCC1-(1–260) was phosphorylated by wild-type SPAK as described in the Materials and methods section. The ^{32}P-labelled NKCC1 was isolated by electrophoresis on a polyacrylamide gel and digested with trypsin, and the resulting peptides were chromatographed on a C_{18} column equilibrated in 0.1 % (v/v) trifluoroacetic acid in water. The column was developed with a linear acetonitrile gradient (diagonal line) at a flow rate of 0.2 ml/min, and fractions (0.1 ml each) were collected. The peak fractions containing the major ^{32}P-labelled peptides are marked as P1 and P2. The indicated peptides were analysed by MALDI–TOF/TOF MS as described in the Materials and methods section. The site of phosphorylation within each peptide was determined by solid-phase Edman sequencing in which ^{32}P radioactivity was measured after each cycle of Edman degradation. The cycle number in which ^{32}P radioactivity was released is indicated. The deduced amino acid sequences of P1 and P2 are indicated in which the phosphorylated residues are underlined. (**B**) As in (**A**), except that wild-type OSR1 was employed in place of SPAK, and the major ^{32}P-labelled peptides are marked as P3 and P4. (**C**) Active [T233E]SPAK was incubated with bacterially expressed wild-type NKCC1-(1–260) or the indicated mutants in the presence of Mg-[γ-^{32}P]ATP. After incubation, the samples were analysed by PAGE and phosphorylation of NKCC1 protein substrate was determined by scintillation counting. NKCC1-TTTAAA corresponds to a mutant in which Thr[175], Thr[179] and Thr[184] were all mutated to alanine. (**D**) As in (**C**), except that active [T185E]OSR1 was employed in place of [T233E]SPAK.

domain were required for interaction with NKCC1 and WNK1, we undertook an alanine scan in which we investigated the effect of mutating 46 residues in CCT domain on its ability to bind to endogenously expressed NKCC1 and WNK1. Most mutations did not affect the binding; however, a few, including those of Asp[479] and Leu[493], disrupted binding of the SPAK CCT domain to both WNK1 and NKCC1 (Figure 4B). We also observed that mutations of other residues, namely Thr[480], Val[484], Glu[487], Val[494], Asp[498] and Val[502] affected binding to NKCC1 to a greater extent than to WNK1 (Figure 4B).

CCT domain of OSR1 is required for efficient phosphorylation of NKCC1

To verify whether removal of the CCT domain affected the intrinsic catalytic activity of OSR1, we first assayed this enzyme with CATCHtide, which does not possess an RFXV motif, and would therefore not be expected to interact directly with the CCT domain. Both full-length [T185E]OSR1 and a mutant of OSR1 lacking the CCT domain ([T185E]OSR1-ΔCCT; residues 1–435) phosphorylated CATCHtide with similar efficiency (Figure 5A), indicating that removal of the CCT domain does not affect the intrinsic OSR1 catalytic activity. We next tested the efficiency with which the [T185E]OSR1-ΔCCT mutant phosphorylated NKCC1, and observed that it was only able to phosphorylate NKCC1-(1–

260) at low background level, similar to that observed with an inactive [T185A]OSR1 mutant. We also investigated how mutations in the CCT domain affected the ability of full-length OSR1 expressed in HEK-293 cells to interact with NKCC1 and WNK1 (Figure 5B). Consistent with the results of the isolated CCT domain, the full-length [T185E/D459A]OSR1, [T185E/V464A]-OSR1 and [T185E/L473A]OSR1 mutants failed to interact with endogenously expressed WNK1 and NKCC1 under conditions in which wild-type OSR1 and [T185E]OSR1 bound strongly (Figure 5B). Moreover, the [T185E/D459A]OSR1, [T185E/V464A]-OSR1 and [T185E/L473A]OSR1 mutants that failed to interact with NKCC1 only phosphorylated NKCC1-(1–260) poorly, while they retained normal catalytic activity towards CATCHtide (Figure 5B).

Characterization of binding properties of the CCT domain

In order to analyse the properties of the CCT domain in more detail, we synthesized a biotinylated peptide that encompasses the RFXV motif on WNK4, proposed to mediate the interaction with SPAK [3]. We investigated the ability of this peptide to interact with wild-type and mutant forms of OSR1, deploying a quantitative BiaCore surface plasmon resonance binding assay. The isolated OSR1 CCT domain interacted with the RFQV (Arg-Phe-Gln-Val) motif-containing peptide with high affinity (apparent K_d
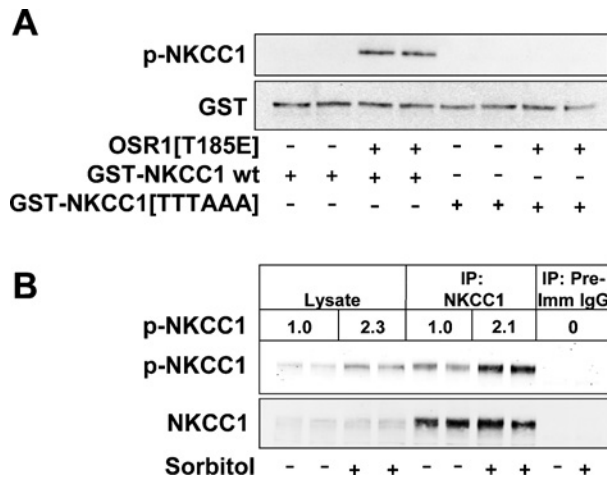
Figure 2   Phosphorylation of endogenous NKCC1

(**A**) The indicated forms of GST–NKCC1-(1–260) were incubated with or without constitutively active [T185E]OSR1 in the presence of MgATP and immunoblotted with anti-phospho-NKCC1 antibody (p-NKCC1) or an anti-GST antibody. (**B**) HEK-293 cells were incubated with or without 0.5 M sorbitol for 30 min and then lysed. Cell lysates (40 μg), or immunoprecipitations (IP) undertaken from 2 mg of lysate with NKCC1 or pre-immune (Pre-Imm) IgG, were analysed by immunoblotting with the anti-phospho-NKCC1 antibody (p-NKCC1) or an antibody raised against NKCC1-(1–260). Similar results were obtained in three separate experiments. Quantification of the phospho-NKCC1 immunoblot was undertaken using the Li-Cor Odyssey® IR imaging system. Results are presented relative to the mean value observed in unstimulated cells, which was given a value of 1.0. OSR1[T185E], GST–[T185E]OSR1; GST-NKCC1 wt, GST–NKCC1-(1–260); GST-NKCC1[TTTAAA], GST–[T175A/T179A/T184A]NKCC1-(1–260).

Figure 3   Generation of a peptide substrate for OSR1

(**A**) Multiple sequence alignment of the indicated fragments of cation–chloride co-transporters encompassing the NKCC1 SPAK and OSR1 sites of phosphorylation, performed using the program T-Coffee [18]. The alignment was graphically represented with BOXSHADE version 3.21 at http://www.ch.embnet.org/software/BOX_form.html using default parameters. Identical residues are highlighted in black and similar residues are in grey. The region of NKCC1 that encompasses CATCHtide is marked with a continuous line, the sites phosphorylated by SPAK and OSR1 are marked with a closed inverted triangle, and the previously identified residues on NKCC1 phosphorylated in cells [13] are marked with closed square. h, human; s, shark. (**B**) Constitutively active GST–[T185E]OSR1 was incubated with the indicated amount of CATCHtide in presence of Mg-[γ-^{32}P]ATP and incorporation of [^{32}P]phosphate into the substrate was determined. Each assay was carried out in triplicate and the results are means $\pm$ S.D. Similar results were obtained in at least three experiments.

of 8 nM; Figure 6A). Several of the CCT domain mutants tested, including [D459A]OSR1, [V464A]OSR1 and [L473A]OSR1, as well as OSR1-ΔCCT, failed to bind the RFQV motif-containing peptide. Other mutants ([V474A]OSR1, [T460A]OSR1) interacted with the RFQV motif-containing peptide with lower affinity than the wild-type CCT domain (Figure 6A). Similar results were obtained when binding of the RFQV motif-containing peptide to these mutants was assessed in a HEK-293 cell lysate peptide pull-down assay (Figure 6B). We next studied how mutation of the RFQV motif affected binding of the peptide to the CCT domain. The AFQV (Ala-Phe-Gln-Val), RAQV (Arg-Ala-Gln-Val) and RFQA (Arg-Phe-Gln-Ala) motif-containing peptides failed to bind the OSR1 CCT domain, whereas the RFAV (Arg-Phe-Ala-Val) motif-containing peptide bound to this domain with an affinity similar to that of the parental RFQV motif-containing peptide (Figure 6C). Employing the biotinylated RFQV or RFAV peptides coupled to streptavidin–Sepharose, we were able to affinity-purify sufficient amounts of endogenously expressed SPAK and OSR1 from 10 mg of HEK-293 cell lysate to visualize them on a Coomassie Blue-stained gel and identify them by MS (Figure 6D). In contrast, we were unable to affinity-purify SPAK and OSR1 using the non-SPAK/OSR1-binding peptides (Figure 6D).

The RFQV peptide did not affect the ability of [T185E]OSR1 to phosphorylate CATCHtide (Figure 7A), indicating that interaction of the CCT domain with an interacting partner does not stimulate kinase activity directly. In contrast, the RFQV peptide suppressed, in a dose-dependent manner, phosphorylation of NKCC1-(1–260) by [T185E]OSR1, establishing further the necessity of the CCT domain in enabling OSR1 to phosphorylate NKCC1 (Figure 7A). Consistent with this, peptides that are unable to bind the CCT domain did not suppress phosphorylation of NKCC1-(1–260) by [T185E]OSR1 (Figure 7B).
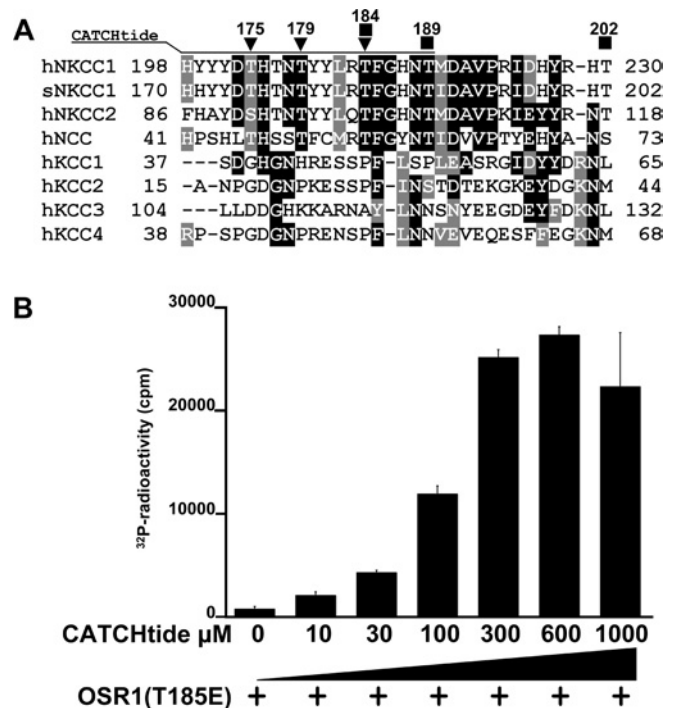
CCT domain facilitates activation of OSR1 by WNK1

We next studied how removal of the CCT domain of OSR1 affected its phosphorylation (Figure 8A) and activation (Figure 8B) by full-length WNK1 *in vitro*. We compared the ability of endogenous WNK1, immunoprecipitated from HEK-293 cell lysates, to phosphorylate full-length OSR1 or OSR1-ΔCCT. WNK1 phosphorylated full-length OSR1 more efficiently than the OSR1-ΔCCT mutant lacking the CCT domain (Figure 8A). In addition, we found that endogenously expressed WNK1 immunoprecipitated from HEK-293 cells activated full-length OSR1 30-fold over a 40 min period (Figure 8B). In contrast, the OSR1-ΔCCT mutant was only activated $\sim$ 10-fold in a parallel experiment (Figure 8B).

DISCUSSION

It is well established that phosphorylation of the N-terminal intracellular regulatory domain of NKCC1 plays a crucial role in regulating the activity of this cation co-transporter [11,12]. *In vivo* ^{32}P-labelling experiments of shark rectal gland tubules identified three phosphorylation sites on NKCC1 (Thr^{184}, Thr^{189} and Thr^{202}) that were stimulated with forskolin and calyculin-A [13]. Mutation of Thr^{189}, but not Thr^{184} and Thr^{202}, was found to inhibit activation of NKCC1 [13]. Another more recent study indicated that the individual mutation of the equivalent sites on
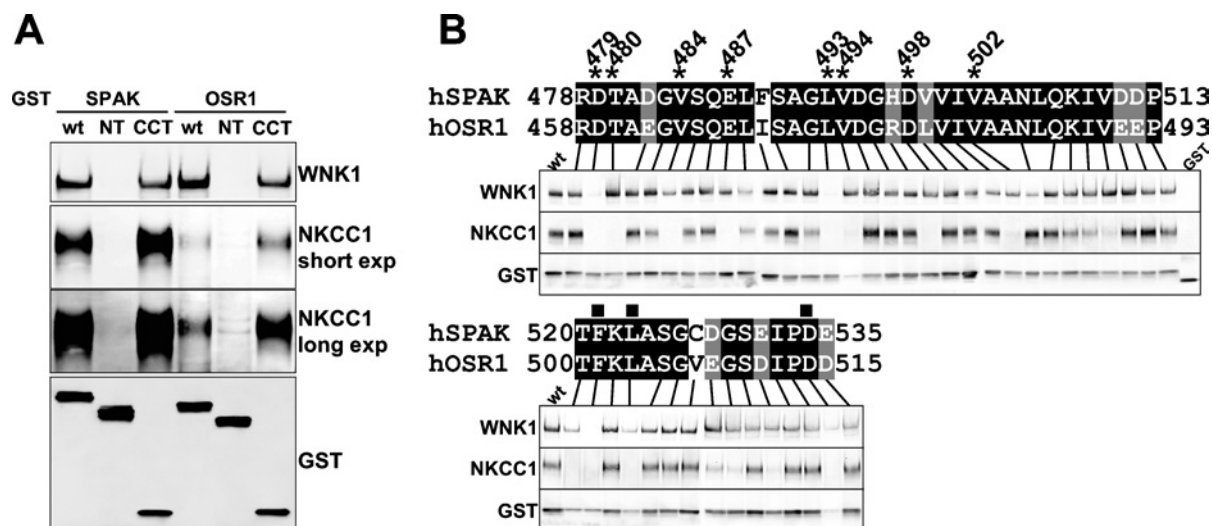
Figure 4   Analysis of the interaction of SPAK and OSR1 with WNK1 and NKCC1

(**A**) HEK-293 cells were transfected with constructs encoding the indicated GST-fusion proteins. At 36 h post-transfection, the GST-fusion proteins were affinity-purified on glutathione–Sepharose beads that were immunoblotted with anti-GST, anti-WNK1 or anti-NKCC1 antibody to detect endogenously associated WNK1 and NKCC1. SPAK wt, full-length GST–SPAK (547 amino acids long); SPAK NT, GST–SPAK-(1–455); SPAK CCT, GST–SPAK-(449–547); OSR1 wt, GST–OSR1 (527 amino acids long); OSR1 NT, GST–OSR1-(1–435); OSR1 CCT, GST–OSR1-(429–527); exp, exposure. (**B**) HEK-293 cells were transfected with constructs encoding the isolated CCT domain of SPAK [GST–SPAK-(449–547)] or the mutants in which the indicated residues had been mutated to alanine. Binding of NKCC1 and WNK1 to these was assessed as above. Residues marked with an asterisk represent mutations that markedly affected binding to NKCC1 and/or WNK1, whereas residues marked with a closed square, although they affected binding to NKCC1 and WNK1, were also found to markedly decrease expression of the isolated CCT domain as well as the full-length protein (results not shown). wt, wild-type.

rabbit NKCC2 did not significantly affect co-transporter activity, but mutation of all three residues markedly inhibited activity [14]. SPAK and OSR1 were originally identified as kinases that interacted with and activated NKCC1 [1,2,4]. Further evidence that SPAK regulates the activity of NKCC1 came from the finding that overexpression of dominant-negative SPAK inhibited NKCC1 phosphorylation and activation [2]. Direct mapping of the residues on NKCC1 that are phosphorylated by SPAK and OSR1 has not previously been undertaken. In the present study, we have demonstrated that SPAK and OSR1 phosphorylate a cluster of three residues on shark NKCC1 (Thr[175], Thr[179] and Thr[184]) and that mutation of all three sites is required to prevent phosphorylation of NKCC1 by SPAK and OSR1 (Figure 1). Importantly, we also established that sorbitol stimulation of cells, which is known to lead to phosphorylation and activation of NKCC1 [11], increases the phosphorylation of NKCC1 at the residues targeted by SPAK and OSR1 in vitro (Figure 2B). Further work will be required to assess the effect that mutation of Thr[175], Thr[179] and Thr[184] has on NKCC1 activity in unstimulated and osmotically stressed cells. In addition, it would be important to establish how inhibition of SPAK/OSR1 and WNK isoforms affects activation and phosphorylation of NKCC1 at the Thr[175], Thr[179] and Thr[184] residues. As mentioned above, only the effect of mutating Thr[184] of NKCC1 has been investigated previously, and its mutation did not substantially affect NKCC1 activity [13,14]. It is therefore possible that phosphorylation of Thr[175] and Thr[179], in addition to Thr[184], contribute to activation of NKCC1 by SPAK and OSR1, and this will need to be verified by further experimentation. Our peptide-mapping studies indicate that Thr[189] and Thr[202] on NKCC1 are not phosphorylated by SPAK and OSR1 in vitro, suggesting that other protein kinase(s) are likely to be targeting those sites in vivo.

The residues in NKCC1 phosphorylated by SPAK and OSR1 as well as the residues surrounding them, are conserved in NKCC2 and NCC (Na⁺–Cl⁻ co-transporter) (Figure 3A). NCC is the target

of the thiazide drugs which effectively lower blood pressure in patients with Gordon's syndrome [7,15]. WNK1 is reportedly overexpressed in humans with mutations in the intronic non-coding region of the *WNK1* gene, indicating that overexpression of WNK1 results in hypertension [7]. Consistent with this notion, heterozygous WNK1^{-/+} mice have lower blood pressure [16]. It would be interesting to investigate the activity of the SPAK/OSR1 kinases, as well as the activity and phosphorylation of NKCC1/2 and NCC, in patients with Gordon's syndrome and WNK1^{-/+} mice. The SPAK and OSR1 phosphorylation sites are not conserved on any of the isoforms of the KCC (K⁺–Cl⁻ co-transporter) family (Figure 3A), suggesting that they may not be controlled in the same manner by SPAK/OSR1. However, KCC3, but not KCC1, KCC2 and KCC4, possesses a putative CCT-binding RFMV (Arg-Phe-Met-Val) motif in a similar position to that found in NKCC1/2 and NCC and this may therefore explain why KCC3 was found to interact with SPAK/OSR1 in a yeast two-hybrid screen [1]. It would be interesting to investigate whether SPAK/OSR1 are capable of phosphorylating and regulating the activity of KCC3.

Our results are consistent with previous studies [1,3,4] indicating that the CCT domain of SPAK and OSR1 interacts with RFXV motifs on NKCC1 as well as WNK1 and WNK4 with high affinity. However, our findings do not exclude the possibility that variants of the RFXV motif might also interact with the CCT domain. It would be of interest to undertake binding analysis employing peptide arrays, in which each of the residues within the RFXV motif was mutated to all of the other amino acids. Our work also defines for the first time a number of mutations in the CCT domain that specifically abolish interaction with NKCC and WNK1. It would be informative to crystallize the CCT domain to define the molecular mechanism by which this domain binds the RFXV motif with high affinity. Our findings in the present study demonstrate for the first time that a functional CCT domain is essential for efficient binding and phosphorylation of the NKCC1
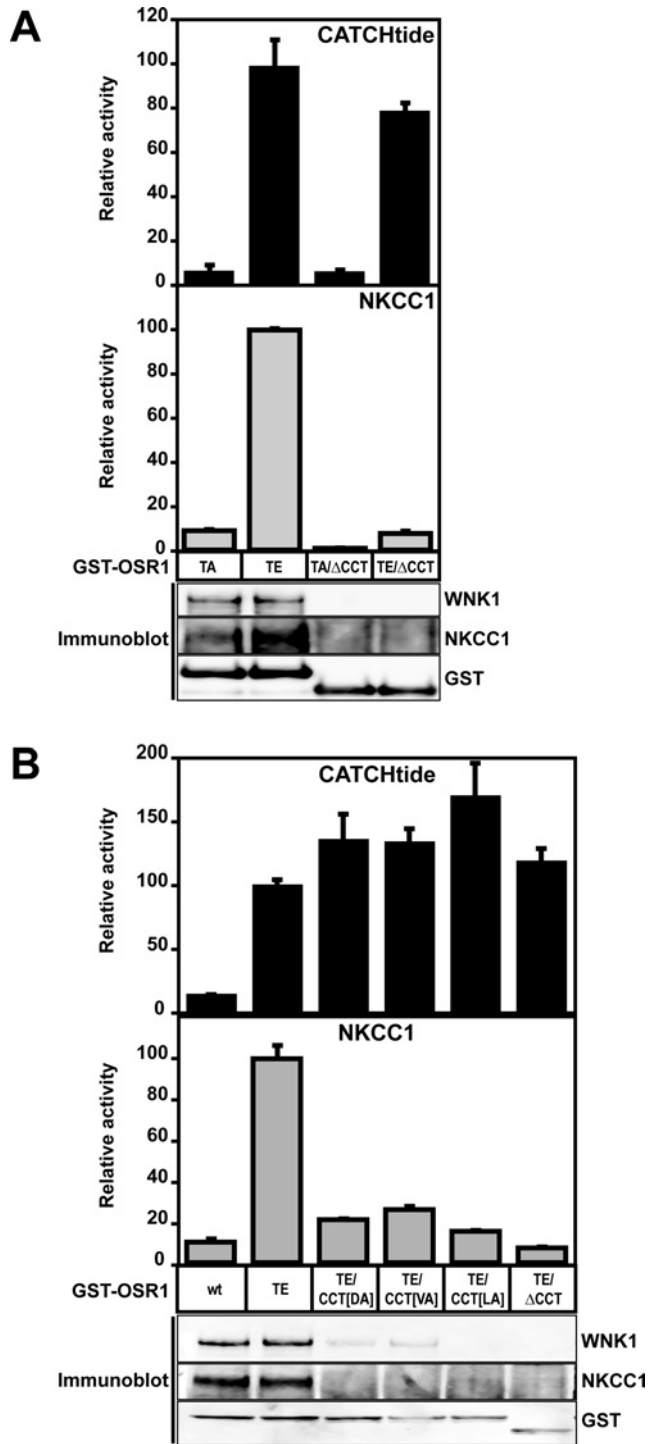
Figure 5   Role of the CCT domain in enabling OSR1 to phosphorylate NKCC1 and CATCHtide

(**A** and **B**) HEK-293 cells were transfected with constructs encoding the indicated mutants of OSR1 as GST-fusion proteins. At 36 h post transfection, the fusion proteins were affinity-purified and incubated with CATCHtide (upper histograms) or sNKCC1-(1–260) (lower histograms) as substrates in the presence of Mg-[γ-^{32}P]ATP, and phosphorylation of these substrates was determined as described in the Materials and methods section. The results are presented relative to the kinase activity observed with GST–[T185E]OSR1, which was given a value of 100. The purified GST–OSR1 proteins were also immunoblotted with indicated antibodies. (**A**) TA, GST–[T185A]OSR1; TE, GST–[T185E]OSR1; TA/△CCT, GST–[T185A]OSR1-△CCT; TE/△CCT, GST–[T185E]OSR1-△CCT. (**B**) wt, GST–OSR1; TE, GST–[T185E]OSR1; TE/ CCT[DA], GST–[T185E/D459A]OSR1; TE/CCT[VA], GST–[T185E/V464A]OSR1; TE/CCT[LA], GST–[T185E/L473A]OSR1, TE/△CCT, GST-[T185E]OSR1-△CCT.
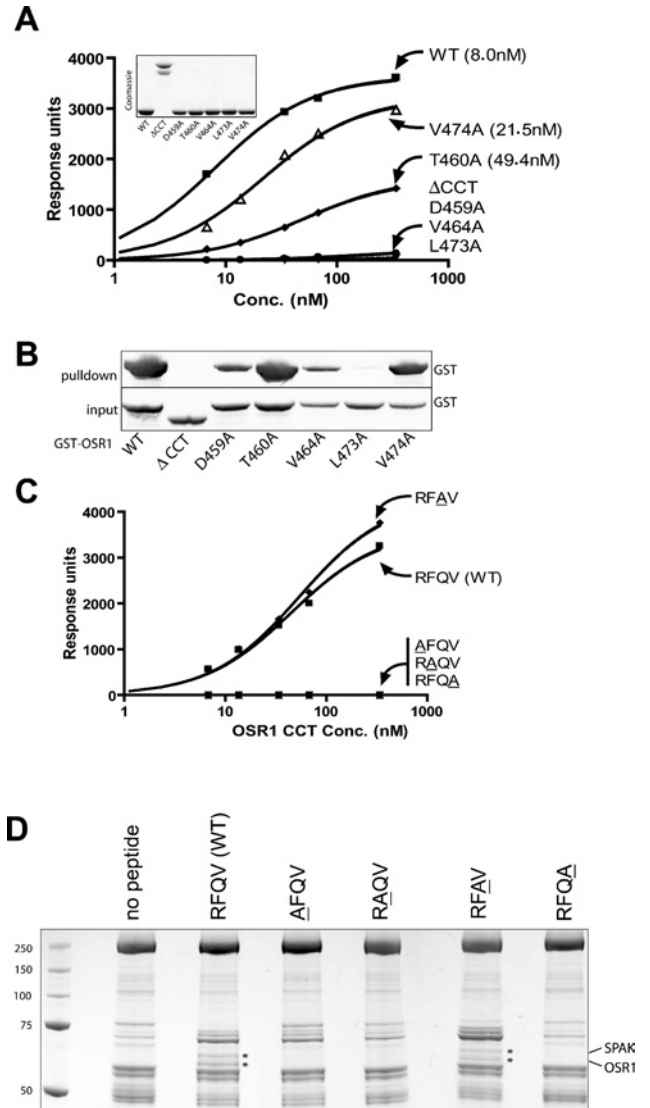

Figure 6   Analysis of the binding properties of the CCT domain

(**A**) The binding of bacterially expressed isolated forms of the OSR1 CCT domain [WT; OSR1-(429–527)] or OSR1-△CCT (residues 1–435) to a biotinylated RFQV motif-containing peptide derived from WNK4 (biotin–SEEGKPQLVGRFQVTSSK) was analysed using BiaCore as described in the Materials and methods section. The analysis was performed over a range of protein concentrations (6.8–340 nM) and the response level at steady state was plotted against the log of the protein concentration. The K_d values were calculated by fitting the data to the equation $y = B_{max} \cdot x/(K_d + x)$ using GraphPad 4 software, which describes the binding of a ligand to a receptor that follows the law of mass action. B_{max} is the maximal binding and K_d is the concentration of ligand required to reach half-maximal binding, whereas x and y correspond to the protein concentration and the response units respectively. The inset shows the similar level of the recombinant proteins employed for this analysis. (**B**) HEK-293 cells were transfected with GST-tagged wild-type (WT) OSR1 or the indicated mutants. At 36 h post-transfection, cells were lysed and subjected to affinity-purification with the biotinylated RFQV peptide as described in the Materials and methods section. The affinity-purified samples (termed pulldown) were immunoblotted with an anti-GST antibody to detect interaction of GST-fusion proteins with the peptide. The cell lysates before affinity-purification (termed input) were also subjected to immunoblotting. (**C**) As in (**A**), except that binding of the isolated OSR1 CCT domain to the indicated biotinylated peptides was determined. The peptide sequences employed are RFQV, biotin–SEEGKPQLVGRFQVTSSK; AFQV, biotin–SEEGKPQLVG_A_FQVTSSK; RAQV, biotin–SEEGKPQLVGR_A_QVTSSK; RFAV, biotin–SEEGKPQLVGRF_A_VTSSK; RFQA, biotin–SEEGKPQLVGRFQ_A_TSSK. Mutated residues are underlined. (**D**) Non-transfected HEK-293 cell lysates were incubated with the biotinylated peptides described in (**C**) and subjected to affinity-purification with streptavidin–Sepharose. The purified samples were analysed on a Coomassie Blue-stained SDS/PAGE gel. The bands marked with an asterisk were subjected to MS fingerprinting and their identity was confirmed as endogenously expressed SPAK and OSR1. Molecular-masses are given in kDa.
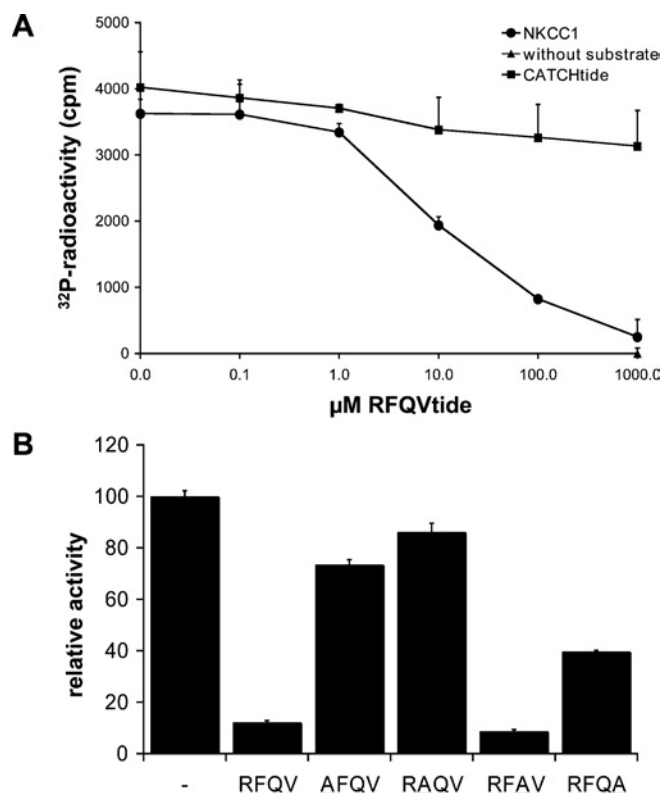
Figure 7   Effects of RFQV motif-containing peptide on OSR1 kinase activity

(**A**) GST–[T185E]OSR1 was incubated with either NKCC1-(1–260) (5 μM) or CATCHtide (10 μM) or alone in the presence of Mg-[γ-^{32}P]ATP and the indicated concentration of RFQV motif-containing peptide. After incubation, the phosphorylation of substrates was determined. Results are means $\pm$ S.D. for a triplicate experiment. Similar results were obtained in two separate experiments. (**B**) As in (**A**), except that samples were incubated with 1 mM of the indicated peptide whose sequence is the same as that described in the legend to Figure 6, except that they were not biotinylated.

substrate by SPAK and OSR1, but not CATCHtide, which does not possess an RPXV motif. These results indicate that the CCT domain functions as a specific substrate-recognition domain, which enables docking of RFXV motif-containing substrates and hence their efficient phosphorylation by SPAK and OSR1. Our results also support the notion that the CCT domain is required for efficient phosphorylation and activation of OSR1 by WNK1, as we observe that the OSR1 mutant lacking the CCT domain is markedly less phosphorylated and activated by full-length WNK1 than the wild-type OSR1 (Figure 8).

Many kinases, such as MAPKs (mitogen-activated protein kinases), GSK3 (glycogen synthase kinase 3) and PDK1 (phosphoinositide-dependent kinase 1), rely on substrate-recognition sites termed docking sites that recognize motifs on their substrate distant from the sites that are phosphorylated (reviewed in [17]). In the MAPKs GSK3 and PDK1, the substrate docking regions are located within a specific pocket of the catalytic domain itself. In contrast, SPAK and OSR1 have evolved a specific relatively large 92-residue domain separate from the kinase domain to interact with substrates as well as upstream regulators. Further work is required to explore how the CCT domain interaction with WNK1 or NKCC1 is co-ordinated in a manner that permits SPAK/OSR1 to become first activated by WNK1/WNK4 and subsequently interact with their substrates. It would also be interesting to determine whether SPAK and OSR1 interact with substrates other than NKCC or other co-transporters through their CCT domain.
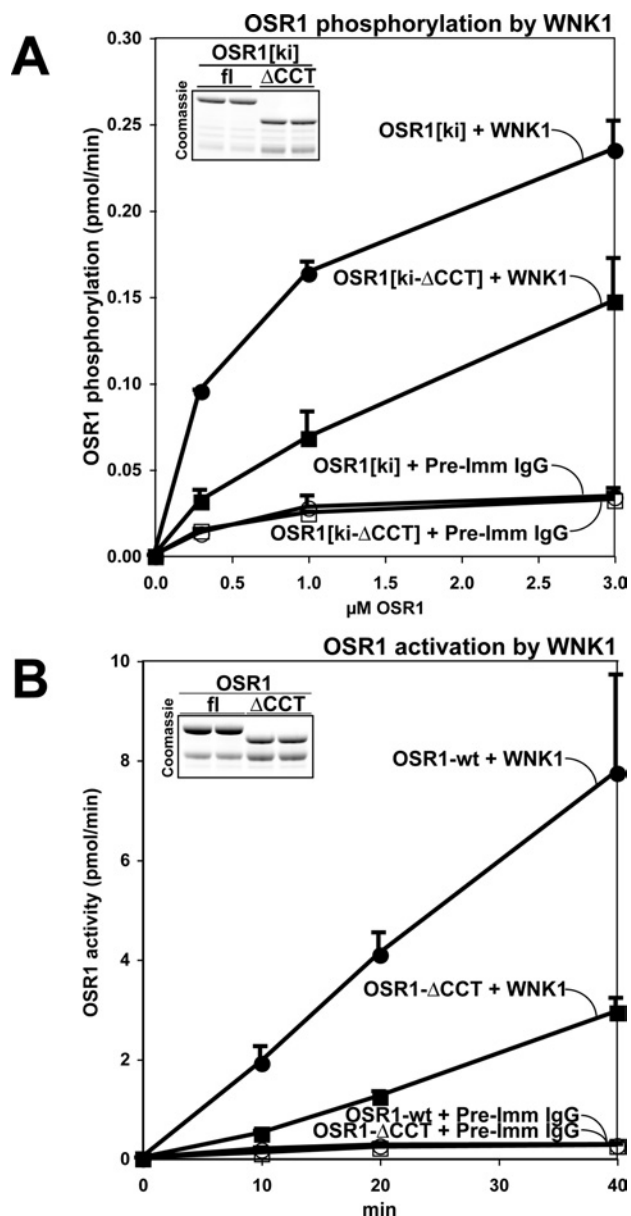

Figure 8   Role of the CCT domain in regulating OSR1 activation by WNK1

(**A**) WNK1 immunoprecipitated from HEK-293 cell lysate (closed symbols) or a control immunoprecipitation performed with pre-immune (Pre-Imm) IgG (open symbols) was incubated in the presence of Mg-[γ-^{32}P]ATP and the indicated concentration of full-length kinase-inactive OSR1[ki] or kinase-inactive OSR1-[ki-ΔCCT] purified from *E. coli*. After incubation, phosphorylation of OSR1 substrate was determined, and results are means $\pm$ S.D. for duplicate experiments. The insert shows a Coomassie Blue-stained SDS/PAGE gel of the purified proteins quantified using a Li-Cor Odyssey$^{®}$ IR imaging system to ensure that a similar molar concentration of full-length OSR1[ki] and mutant OSR1[ki-ΔCCT] were employed in the assay. OSR1[ki] or fl, full-length [D164A]OSR1; OSR1[ki-ΔCCT] or ΔCCT, [D164A]OSR1-ΔCCT. (**B**) Full-length GST-OSR1 or GST–OSR1-ΔCCT purified from *E. coli* were incubated with either WNK1 immunoprecipitated from HEK-293 cell lysate (closed symbols) or with a control immunoprecipitation performed with pre-immune (Pre-Imm) IgG antibody (open symbols), in the presence of CATCHtide and Mg-[γ-^{32}P]ATP. After the indicated time of incubation, phosphorylation of CATCHtide was determined and results are mean $\pm$ S.D. activities for triplicate experiments. The inset shows a Coomassie Blue-stained SDS/PAGE gel of the purified GST-fusion proteins quantified using a Li-Cor Odyssey$^{®}$ IR imaging system to ensure that a similar molar concentration of wild-type OSR1 and mutant OSR1-ΔCCT were employed in the activity assay. Recombinant OSR1 migrates as a doublet band with the upper band migrating with the expected molecular mass. We presume that the lower band is a proteolytic fragment containing the kinase domain and lacking the C-terminal portion, as these enzymes were expressed as N-terminal GST-fusion proteins. OSR1-wt or fl, wild-type GST–OSR1; OSR1-ΔCCT or ΔCCT, GST–OSR1-ΔCCT.

REFERENCES

1 Piechotta, K., Lu, J. and Delpire, E. (2002) Cation chloride cotransporters interact with the stress-related kinases Ste20-related proline-alanine-rich kinase (SPAK) and oxidative stress response 1 (OSR1). J. Biol. Chem. **277**, 50812–50819

2 Dowd, B. F. and Forbush, B. (2003) PASK (proline-alanine-rich STE20-related kinase), a regulatory kinase of the Na–K–Cl cotransporter (NKCC1). J. Biol. Chem. **278**, 27347–27353

3 Gagnon, K. B., England, R. and Delpire, E. (2006) Volume sensitivity of cation–Cl⁻ cotransporters is modulated by the interaction of two kinases: Ste20-related proline-alanine-rich kinase and WNK4. Am. J. Physiol. Cell Physiol. **290**, C134–C142

4 Piechotta, K., Garbarini, N., England, R. and Delpire, E. (2003) Characterization of the interaction of the stress kinase SPAK with the Na⁺–K⁺–2Cl⁻ cotransporter in the nervous system: evidence for a scaffolding role of the kinase. J. Biol. Chem. **278**, 52848–52856

5 Moriguchi, T., Urushiyama, S., Hisamoto, N., Iemura, S., Uchida, S., Natsume, T., Matsumoto, K. and Shibuya, H. (2005) WNK1 regulates phosphorylation of cation–chloride-coupled cotransporters via the STE20-related kinases, SPAK and OSR1. J. Biol. Chem. **280**, 42685–42693

6 Vitari, A. C., Deak, M., Morrice, N. A. and Alessi, D. R. (2005) The WNK1 and WNK4 protein kinases that are mutated in Gordon's hypertension syndrome, phosphorylate and activate SPAK and OSR1 protein kinases. Biochem. J. **391**, 17–24

7 Wilson, F. H., Disse-Nicodeme, S., Choate, K. A., Ishikawa, K., Nelson-Williams, C., Desitter, I., Gunel, M., Milford, D. V., Lipkin, G. W., Achard, J. M. et al. (2001) Human hypertension caused by mutations in WNK kinases. Science **293**, 1107–1112

8 Vitari, A. C., Deak, M., Collins, B. J., Morrice, N., Prescott, A. R., Phelan, A., Humphreys, S. and Alessi, D. R. (2004) WNK1, the kinase mutated in an inherited high-blood-pressure syndrome, is a novel PKB (protein kinase B)/Akt substrate. Biochem. J. **378**, 257–268

9 Campbell, D. G. and Morrice, N. A. (2002) Identification of protein phosphorylation sites by a combination of mass spectrometry and solid phase Edman sequencing. J. Biomol. Tech. **13**, 121–132

10 Alessi, D. R., Cohen, P., Ashworth, A., Cowley, S., Leevers, S. J. and Marshall, C. J. (1995) Assay and expression of mitogen-activated protein kinase, MAP kinase kinase, and Raf. Methods Enzymol. **255**, 279–290

11 Lytle, C. and Forbush, 3rd, B. (1992) The Na–K–Cl cotransport protein of shark rectal gland. II. Regulation by direct phosphorylation. J. Biol. Chem. **267**, 25438–25443

12 Kurihara, K., Moore-Hoon, M. L., Saitoh, M. and Turner, R. J. (1999) Characterization of a phosphorylation event resulting in upregulation of the salivary Na⁺–K⁺–2Cl⁻ cotransporter. Am. J. Physiol. **277**, C1184–C1193

13 Darman, R. B. and Forbush, B. (2002) A regulatory locus of phosphorylation in the N terminus of the Na–K–Cl cotransporter, NKCC1. J. Biol. Chem. **277**, 37542–37550

14 Gimenez, I. and Forbush, B. (2005) Regulatory phosphorylation sites in the NH₂ terminus of the renal Na–K–Cl cotransporter (NKCC2). Am. J. Physiol. Renal Physiol. **289**, F1341–F1345

15 Gordon, R. D. and Hodsman, G. P. (1986) The syndrome of hypertension and hyperkalaemia without renal failure: long term correction by thiazide diuretic. Scott. Med. J. **31**, 43–44

16 Zambrowicz, B. P., Abuin, A., Ramirez-Solis, R., Richter, L. J., Piggott, J., BeltrandelRio, H., Buxton, E. C., Edwards, J., Finch, R. A., Friddle, C. J. et al. (2003) Wnk1 kinase deficiency lowers blood pressure in mice: a gene-trap screen to identify potential targets for therapeutic intervention. Proc. Natl. Acad. Sci. U.S.A. **100**, 14109–14114

17 Biondi, R. M. and Nebreda, A. R. (2003) Signalling specificity of Ser/Thr protein kinases through docking site-mediated interactions. Biochem. J. **372**, 1–13

18 Rice, P., Longden, I. and Bleasby, A. (2000) EMBOSS: the European Molecular Biology Open Software Suite. Trends Genet. **16**, 276–277